



ISSN 0975-413X
CODEN (USA): PCHHAX

Der Pharma Chemica, 2016, 8(13):214-230
(<http://derpharmachemica.com/archive.html>)

Effect of some imidazopyridine compounds on carbon steel corrosion in hydrochloric acid solution

E. Ech-chihbi^{1,2}, R. Salim^{1,2}, H. Oudda², A. Elaattiaoui³, Z. Rais¹, A. Oussaid,
F. El Hajjaji^{1*}, B. Hammouti³, H. Elmsellem³ and M. Taleb¹

¹Laboratoire des Procédés de Séparation, Faculté des Sciences, Kenitra (LPS), Université Ibno Tofail Maroc.

²Laboratoire d'Ingénierie d'Electrochimie, Modélisation et d'Environnement (LIEME), Faculté des sciences/Université Sidi Mohammed Ben Abdellah, Fès, Maroc.

³Laboratoire de chimie analytique appliquée, matériaux et environnement (LC2AME), Faculté des Sciences, B.P. 717, 60000 Oujda, Morocco.

ABSTRACT

The corrosion inhibition of C38 steel in molar hydrochloric acid solution with different concentrations by three newly synthesized imidazopyridine derivatives namely: was studied using gravimetric, potentiodynamic polarization (PP) and electrochemical impedance spectroscopy (EIS) measurements. All compounds have shown good inhibition efficiency (IE %) in acidic solution range 86.5-92.5% for 10-3M at 298K, this efficiency decreased with decreasing the inhibitors concentration and also decreases with increasing temperature. Potentiodynamic polarization studies suggested that the imidazopyridine derivatives mixed-type inhibitors and impedance measurements showed that the double layer capacitance (Cd) increased with rise concentration of the studied inhibitors. The compounds were adsorbed according to the Langmuir isotherm and the inhibition influenced by hemis- and chemi-sorption. Some thermodynamic functions of adsorption and dissolution process were calculated and discussed.

Keywords: Imidazopyridine; efficiency; Inhibition; Hydrochloric acid; Adsorption.

INTRODUCTION

Hydrochloric acid (HCl) solutions are a highly corrosive to any metals generally used in many industrial processes such as the pickling of metals. Use of inhibitors is one of the most economical methods to mitigate the corrosion rate with the metal surface, especially in acid solutions [1-3]. The inhibitors can form a protective barrier on the metal surface against corrosive agents in blocking either anodic or cathodic sites. The corrosion inhibition efficiency depends on the adsorption properties and generally affected by the interaction of π -orbitals of the inhibitors with d-orbitals of the surface atoms [4], functional group, steric factors aromaticity and the electronic density of the donor atoms [5-7].

In general, the organic compounds have demonstrated that the compounds that have nitrogen and sulfur in their structure adduce a greater inhibition than those than only contain one of the atoms at a time, being this property attributable to its molecular structure [8]. The organic molecules used as inhibitors, especially aromatic molecules containing electronegative functional groups and π electrons or conjugated double or triple bonds [9] and presence of heteroatoms such as nitrogen, sulfur and/or oxygen atoms [10-13].

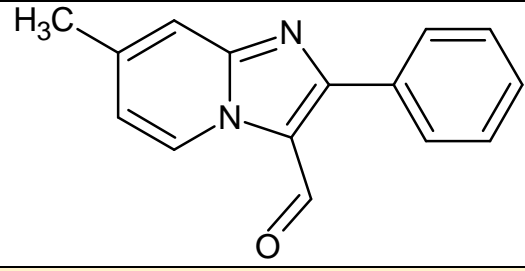
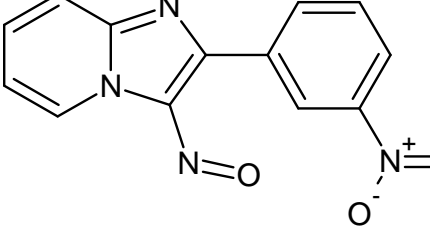
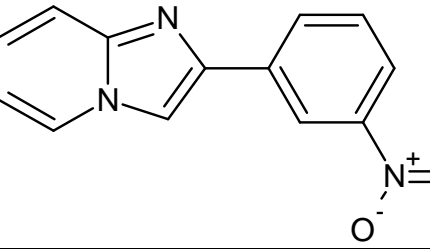
Imidazo [1, 2-a] pyridine derivatives are of interest because of their potential analgesic, anti-inflammatory, antipyretic, anticonvulsant, [14]

Some derivatives of imidazole [15–17] have been reported as excellent inhibitors for metals and alloys in hydrochloric acid solution and exhibit different inhibition performance with the difference in substituent groups and substituent positions on the aromatic rings. This can be interpreted that in imidazopyridine derivatives molecules show anchoring sites suitable for bonding with the metal surface. So, it was expected that imidazopyridine derivatives would work as a good corrosion inhibitor for mild steel in hydrochloric acid solution.

The objective of this study is to evaluate the corrosion inhibition efficiency of carbon steel in 1M at different concentrations as well as temperatures by: 2-(3-nitrophenyl)-6-methylimidazo[1,2-a]pyridine, 2-(3-nitrophenyl)-3-nitrosoimidazo[1,2-a]pyridine and 2-(3 nitrophenyl) imidazo [1,2-a]pyridine denoted hereafter P1, P2 and P3 respectively. Table 1 shows the molecular structures of the organic compounds [18]. Weight loss, Potentiodynamic polarization (PP) and electrochemical impedance spectroscopy (EIS) measurements were used in this study. The thermodynamic and kinetic parameters were determined and discussed, also the adsorption mechanism of the studied inhibitors.

The inhibitors P1, P2, and P3 were synthesized in the laboratory by a reported method [18]

Table 1: Molecular structures, names and abbreviations of the studied of the studied imidazopyridine compounds

Compound	Imidazopyridine Formula	Abbreviation
1		P1
Name	2-(3-nitrophenyl)-6-methylimidazo[1,2-a]pyridine	
2		P2
Name	2-(3-nitrophenyl)-3-nitrosoimidazo[1,2-a]pyridine	
3		P3
Name	2-(3 nitrophenyl) imidazo [1,2-a]pyridine	

MATERIALS AND METHODS

The metal used in this study is a carbon steel C38 with a chemical composition in wt. % 0.21 C; 0.38 Si; 0.09 P; 0.01 Al; 0.05 Mn; 0.05 S. the steel plates were mechanically abraded successively by emery papers of different grit size, ranging from 180 to 1500 grades the surface was rinsing by distilled water and degreasing in acetone followed by drying. The acid solution of HCl 1M was prepared dilution of analytical grade 37% HCl with distilled water.

2.2. Weight loss measurements

Weight loss measurements were performed at 298 K for 6 h and at temperature range of 303 K to 333 K for two hours by immersing the carbon steel coupons into acid solutions.

The measurements were carried out for the uninhibited solution (blank) and solutions containing inhibitor. The inhibition efficiency (IE%) was determined by using following Eq. (1) [19]:

$$IE\% = \frac{W_{corr} - W'_{corr}}{W_{corr}} * 100 \quad (1)$$

Where W_{corr} and W'_{inh} are the values of the corrosion rate in the absence and presence of inhibitor respectively.

2.3. Electrochemical measurements

The electrochemical tests were performed with three-electrode (Pt counter electrode, a CSE reference electrode and a carbon steel working electrode WE), connected to a potentiostat radiometer analytical type PGZ 100 driven by an analysis software "Volta lab Master 4". 1cm^2 of the WE surface is in contact with the solution test for 30min to reach a steady state open circuit potential E_{ocp} . After reaching E_{ocp} , the potential was starting from E_{ocp} and moving to a more positive potential (anodic reaction) or negative potential (cathodic reaction) at a scan rate of 1 mV/s. The linear Tafel segments of anodic and cathodic curves were extrapolated potential to obtain corrosion current densities I_{corr} . The inhibition efficiencies were calculated using the Eq. (2) [20]:

$$IE\% = \frac{I_{corr} - I'_{corr}}{I_{corr}} * 100 \quad (2)$$

Where I_{corr} and I'_{inh} are the values of the corrosion current densities in the absence and presence of inhibitor respectively.

The Electrochemical Impedance Spectroscopy (EIS) experiments were conducted in the frequency range from 100 KHz to 10 MHz with alternating current amplitude of $\pm 10\text{mV}$.

The impedance diagrams are given in the Nyquist representation. The inhibition efficiency was calculated from charge transfer resistance from the equation (3) [19]:

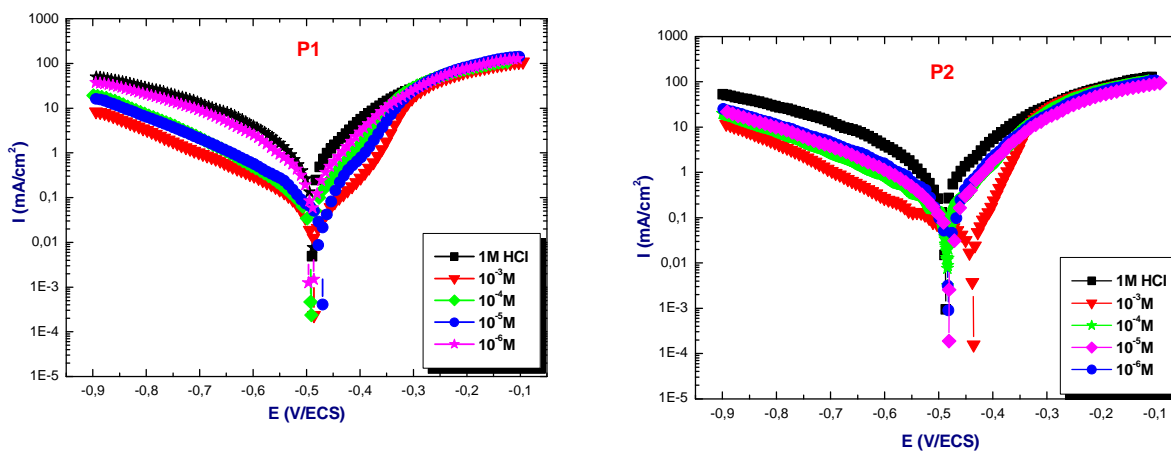
$$IE\% = \frac{R_{tc/inh} - R_{tc}}{R_{tc/inh}} * 100 \quad (3)$$

Where $R_{tc/inh}$ and R_{tc} are the charge transfer resistance values with and without inhibitor, respectively.

RESULTS AND DISCUSSION

3.1 Polarization curves

The effect of rise concentration of compounds P1, P2 and P3 on the anodic and cathodic polarization curves of carbon steel in molar hydrochloric is presented in Figure1.



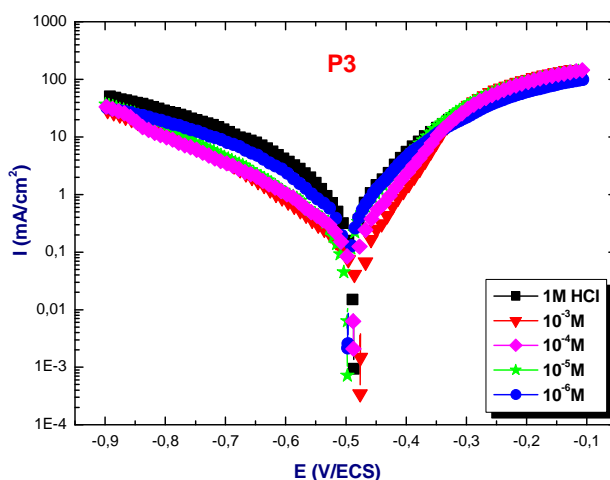


Figure 1. Potentiodynamic polarization curves in 1M HCl, obtained at 298 K without and with addition of the inhibitors at different concentrations

From these results we can conclude that the addition of the compounds studied reduced the cathodic current density, and this decreasing is more marked for the concentration of 10^{-3} M. Cathodic polarization curves present a linearity range indicating that the discharge of proton H^+ is activation-controlled. The Tafel slope variations suggest that benzimidazopyridine compounds influence the kinetics of the hydrogen evolution reaction [21-23]. This stipulates that the inhibitors adsorbed on the cathode and anode site of steel which suggests that these compounds could be classified as mixed-type inhibitors with a cathodic predominance. We also remark that the polarization curves are shifted toward more negative potential values confirming the mixed nature of these inhibitors [24]. It is also observed that for potentials higher than $-350 mV_{ESC}$, the compounds start to be desorbed.

The values of corrosion potential (E_{corr}), cathodic Tafel slope (β_c), corrosion current density (I_{corr}) and the inhibition efficiency (IE%) are shown in Table 2.

Table 2 shows that the values of i_{corr} decreased with increasing inhibitors concentration. The displacement of E_{corr} is less than 85 mV for all inhibitors, which confirms the mixed character of these compounds [25]. The inhibition efficiency of these compounds follows the sequence $P2 > P1 > P3$ for the various concentrations used. This behavior can be attributed to the presence of free electron donating (O, N, π -electrons). Also the mesomeric effect of group (C = N-O) and (C = C-C = O) favors good adsorption of molecules P2 and P1 compared P3.

Table 2. Polarization parameters for carbon steel in molar hydrochloric evaluated from the cathodic of various concentrations of inhibitors P1, P2, and P3

Inhibitors	Concentration (M)	E (V/ECS)	I_{corr} ($mA \cdot cm^{-2}$)	Bc ($mV \cdot dec^{-1}$)	IE (%)
1M HCl	--	-0,486	0,726	158,8	--
P1	10^{-3}	-0,482	0,072	153,5	90,08
	10^{-4}	-0,467	0,080	160,6	88,98
	10^{-5}	-0,488	0,085	146,1	88,19
	10^{-6}	-0,485	0,292	158,4	59,69
P2	10^{-3}	-0,434	0,056	161,2	92,25
	10^{-4}	-0,483	0,139	157,0	81,91
	10^{-5}	-0,480	0,171	160,0	76,46
	10^{-6}	-0,481	0,243	152,1	66,50
P3	10^{-3}	-0,475	0,095	161,3	86,80
	10^{-4}	-0,497	0,239	170,3	68,05
	10^{-5}	-0,488	0,308	171,0	58,33
	10^{-6}	-0,497	0,752	167,2	22,22

3.2. Electrochemical Impedance Spectroscopy

Figure 2. Shows the Nyquist plots for carbon steel C38 in 1M HCl in the absence and presence of different concentration of P1, P2 and P3 at 298K.

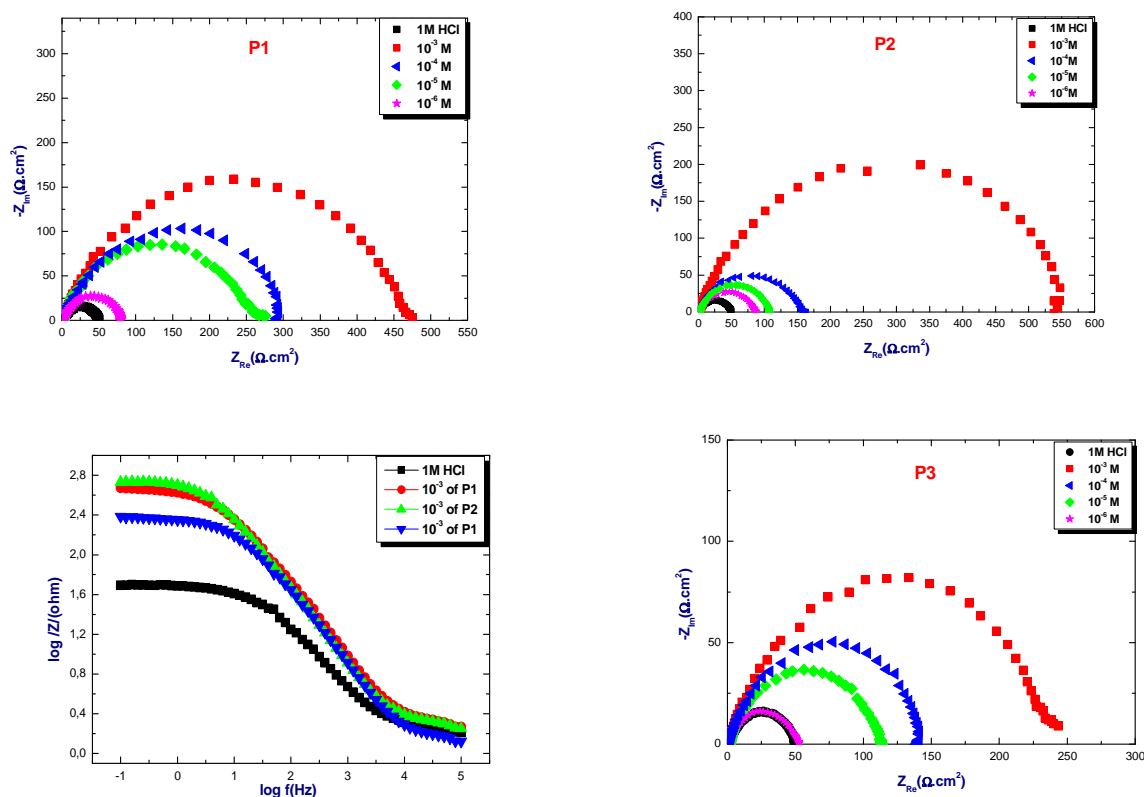


Figure 2. Nyquist diagram for carbon steel in 1M HCl, obtained at 298 K without and with addition of the inhibitors at concentrations ranging from 10^{-6} to 10^{-3} M

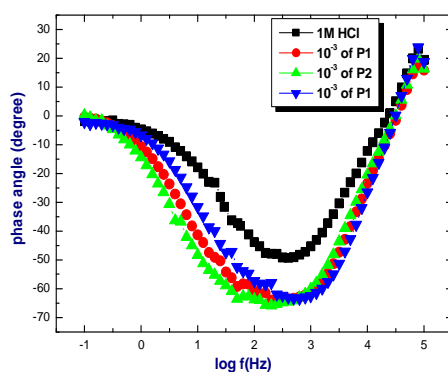


Figure 3. Bode diagrams for carbon steel in 1M HCl, obtained at 298 K without and with addition of the inhibitors at concentrations 10^{-3} M

The Nyquist impedance diagrams obtained are not perfect semi-circles, and this is attributed to the frequency dispersion of interfacial impedance as a result of the no homogeneity or roughness of the metal surface. The diameter of the capacitive loop in the presence of inhibitor is greater than that of the blank solution, and enlarges with increasing inhibitor concentration, which may be attributed to the charge transfer process.

The bode diagrams and phase angle curves for carbon steel in 1M HCl without and with various concentrations of inhibitors are displayed in (Figure 3). Show that the impedance value in the presence of inhibitor is larger than the

blank test and fall to zero at high frequency region. These mean that the corrosion rate is reduced in the presence of the corrosion inhibitors, at a fixed inhibitor concentration 10^{-3} M, following the order: P2 > P1 > P3, confirming the highest inhibitive influence of compounds P2 and P1. Based on shifting trend of phase the angle plots, raising the concentration of inhibitors contributes to more negative values of the phase angle, indicating the better inhibition ability of inhibitors with higher concentrations.

Table 3 summaries the characteristic kinetic parameters associated to the impedance study such as the charge-transfer resistance R_{ct} , the double layer capacitance C_{dl} and the inhibiting efficiency IE%. The charge-transfer resistance (R_{ct}) values are calculated from the difference in impedance at lower and higher frequencies [26]. Whereas, the double layer capacitance (C_{dl}) and the frequency at which the imaginary component of the impedance is maximal ($-Z_{max}$) are found as represented in equation (Eq. 4).

$$C_{dl} = \frac{1}{\omega R_{ct}} \quad \text{Where} \quad \omega = 2\pi f_{max} \quad (4)$$

Table 3. Impedance parameters evaluated in for carbon steel of various concentrations of the studied benzoimidazopyridine molecules

Inhibitors	Concentration (M)	R_t ($\Omega \cdot \text{cm}^2$)	C_{de} ($\mu\text{F}/\text{cm}^2$)	f_{max} (Hz)	IE (%)
Blank	--	48	290	16.24	--
P1	10^{-3}	480	53.6	159.04	90,00
	10^{-4}	294	96.5	85.36	83,67
	10^{-5}	264	98.7	103.34	81,81
	10^{-6}	80	130.5	94.73	40,00
P2	10^{-3}	552	50.9	229.7	91,30
	10^{-4}	170	120	49.05	71.76
	10^{-5}	106	135	36.24	54.71
	10^{-6}	86	160	27.87	44.18
P3	10^{-3}	240	102	82.15	80,00
	10^{-4}	141	109	50.4	65.95
	10^{-5}	112	115	36.6	57.14
	10^{-6}	51	280	17.0	5.88

The inhibitory efficiency increases with the concentration of the inhibitor to attain maximum values of 90, 91.3 and 80% to 10^{-3} M. The values R_{ct} and C_{dl} are also brought down to the maximum extent with the increasing of inhibitors concentration. The decrease of C_{dl} may result from a decrease in the local dielectric constant and / or an increase in the thickness of the double electric suggests that these compounds function by adsorption to metal interface [27].

The impedance of the Nyquist plots were analyzed by fitting the experimental data to a simple equivalent circuit model is given in Figure 4. Which includes the solution resistance R_s and the double layer capacitance C_{dl} which is placed in parallel to the charge transfer resistance R_{ct} .

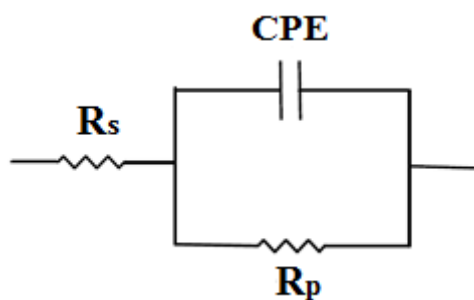


Figure 4. Equivalent electrical circuit model corresponding to the corrosion process on the carbon steel in hydrochloric acid

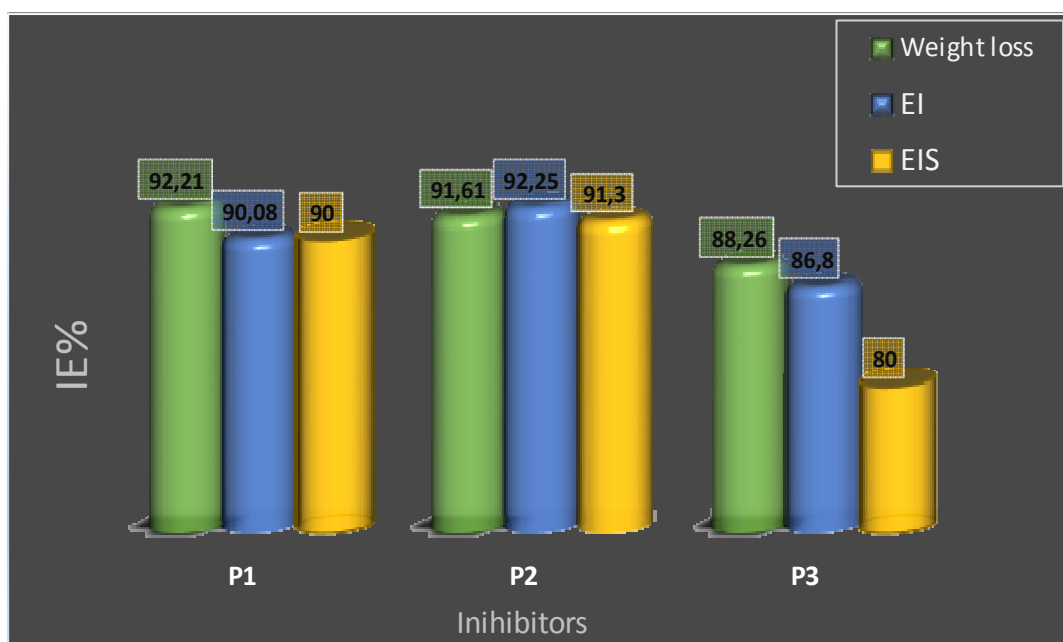


Figure 5. Comparison of inhibition efficiency (IE %) values obtained by weight loss, EI and EIS methods

3.3. Weight loss measurements

3.3.1. Thermodynamic activation parameters

The effect of temperature is very important to study the interaction between C38 steel and the acidic solution. Weight loss measurements were taken at various temperature (308-338K) in the absence and the presence of 2-(3-nitrophenyl)-6-methylimidazo[1,2-a]pyridine (P1) 2-(3-nitrophenyl)-3-nitrosoimidazo[1,2-a]pyridine (P2) and 2-(3 nitrophenyl) imidazo [1,2-a]pyridine (P3) during a period of 2 hours at different concentrations. Results obtained are given in table 4.

Table 4. Influence of temperature on the corrosion rate of mild steel in the presence and absence of inhibitors P1, P2 and P3 at various concentration for 2h immersion time

Temperature (K)	Concentration (M)	P1		P2		P3	
		W_{corr} (mg cm ⁻² h ⁻¹)	IE (%)	W_{corr} (mg cm ⁻² h ⁻¹)	IE (%)	W_{corr} (mg cm ⁻² h ⁻¹)	IE (%)
308	--	1,2181	--	1,2181	--	1,2181	--
	10 ⁻³	0,1142	90,61	0,1142	90,61	0,2409	80,22
	10 ⁻⁴	0,2679	78,00	0,2500	79,46	0,4443	63,52
	10 ⁻⁵	0,3632	70,18	0,2917	76,04	0,4855	60,13
	10 ⁻⁶	0,6246	48,72	0,4952	59,34	0,9643	20,83
318	--	1,7963	--	1,7963	--	1,7963	--
	10 ⁻³	0,2495	86,10	0,2130	88,14	0,4077	77,30
	10 ⁻⁴	0,6531	63,63	0,5273	70,64	0,8791	51,05
	10 ⁻⁵	0,6850	61,86	0,6177	65,60	0,9080	49,45
	10 ⁻⁶	1,0391	42,14	1,0159	43,44	1,4808	17,56
328	--	2,773	--	2,773	--	2,773	--
	10 ⁻³	0,5932	78,60	0,6056	78,15	0,6950	74,93
	10 ⁻⁴	1,2726	54,10	0,9771	64,76	1,6747	39,60
	10 ⁻⁵	1,3955	49,67	1,0887	60,73	1,9214	30,71
	10 ⁻⁶	1,8936	31,71	1,6812	39,37	2,3346	15,80
338	00	4,165	--	4,165	--	4,165	--
	10 ⁻³	1,1861	71,52	1,2451	70,10	1,5815	62,02
	10 ⁻⁴	2,3762	42,94	1,9430	53,34	2,8341	31,95
	10 ⁻⁵	2,4958	40,07	2,1546	48,26	3,1214	25,05
	10 ⁻⁶	3,0760	26,14	3,1385	24,64	3,7387	10,23

From these results, the corrosion rates increase rise of temperature. This increase is more rapidly in the absence of inhibitors in less concentration of the studied molecules when compared to those at higher concentrations. Whereas an opposite evolution is registered for the last two concentrations at a fixed temperature. Apparently, the results postulate that all his inhibitors by adsorption onto the metal surface blocking the active sites to form a barrier on the metal surface against the infiltration of the acid solution. The increase in temperature causes the desorption of the inhibitors studied from the surface of the mild steel.

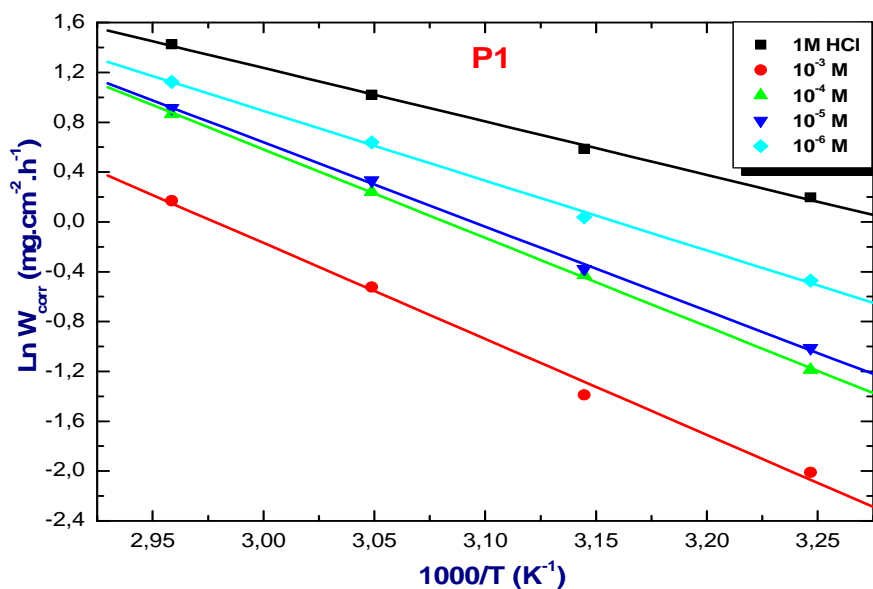
Activation parameters like activation energy (E_a), enthalpy (ΔH^*), and entropy (ΔS^*) for the dissolution of mild steel in 1 M HCl in the absence and presence of various concentrations of P1, P2 and P3 were calculated from the Arrhenius equation (Eq.5) and its alternative formulation called transition state equation (Eq.6):

$$W_{\text{corr}} = A e^{\left(\frac{-E_a}{RT}\right)} \quad (5)$$

$$W = \frac{RT}{Nh} \exp\left(\frac{\Delta S^*}{R}\right) \exp\left(-\frac{\Delta H^*}{RT}\right) \quad (6)$$

Where T is the absolute temperature, A is a constant and R is the universal gas constant, N is Avogadro's number, h is the Planck's constant ($h = 6.6252 \cdot 10^{-34}$ J.s), ΔH^* and ΔS^* are the activation enthalpy and the entropy activation of corrosion process, respectively.

The activation energy E_a is calculated from the slope of the plots of the weight-loss ($\ln W_{\text{corr}}$) versus ($1000/T$), for mild steel in the corrosive medium with and without addition of inhibitors (Figure 6). ($\ln W_{\text{corr}}/T$) vs. ($1000/T$) give straight lines with slopes of ($\Delta H^*/R$) and intercepts of ($\ln(R/Nh) + \Delta S^*/R$) as shown in Figure 6. From equation 5, the values of ΔH^* and ΔS^* can be calculated.



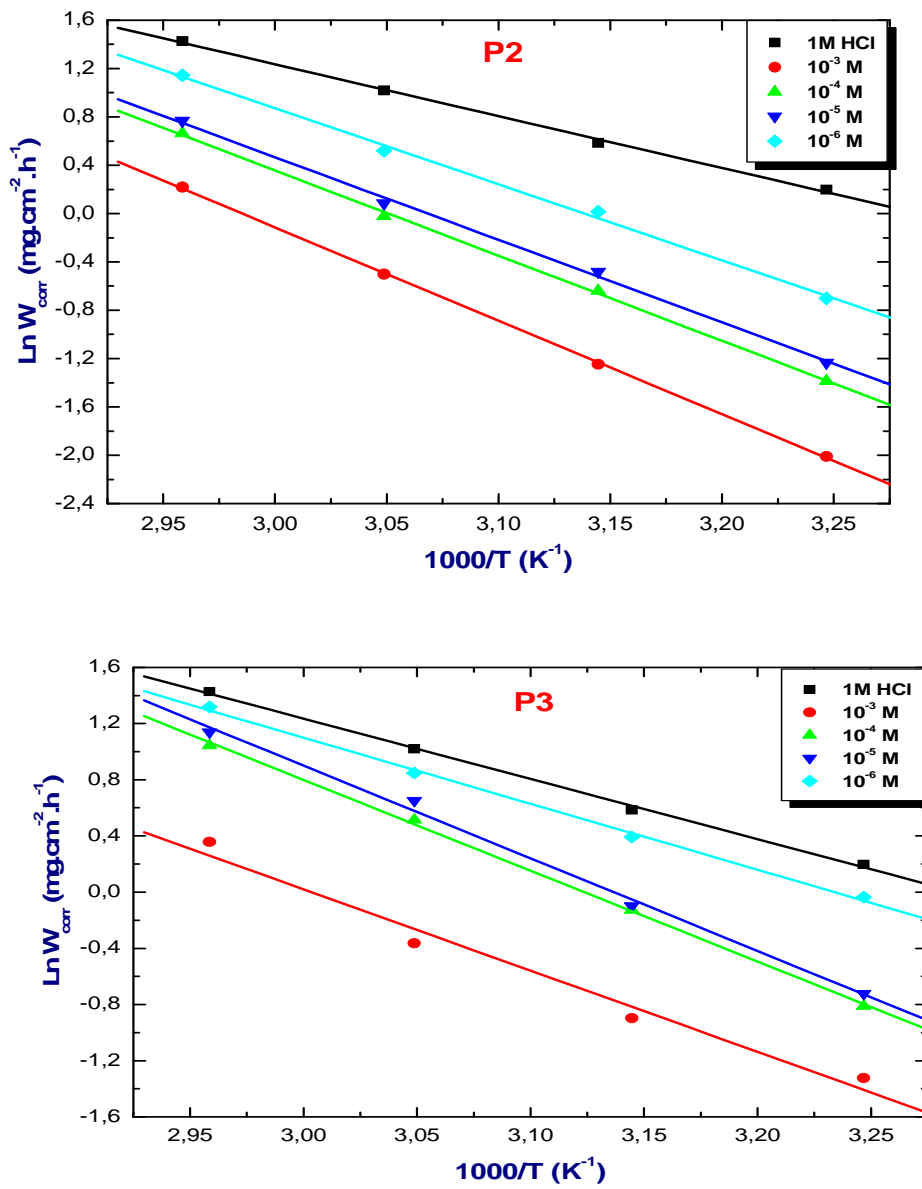
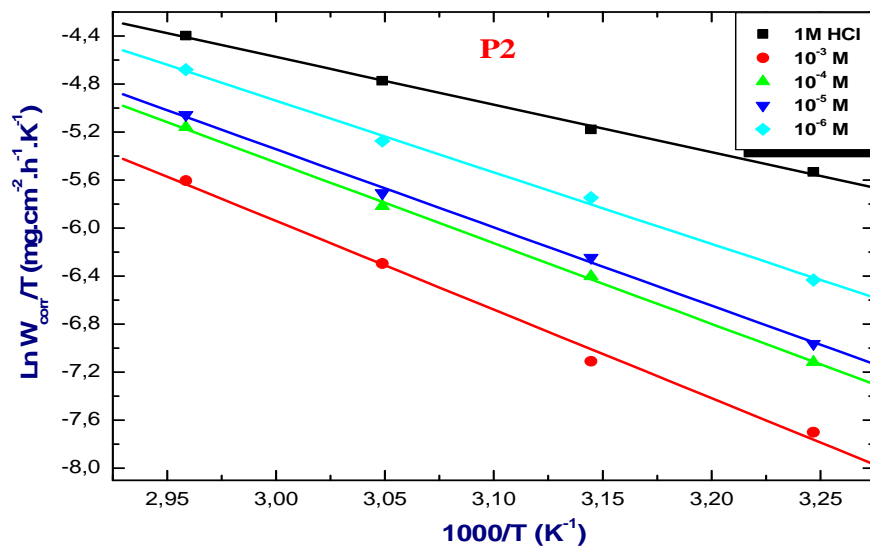
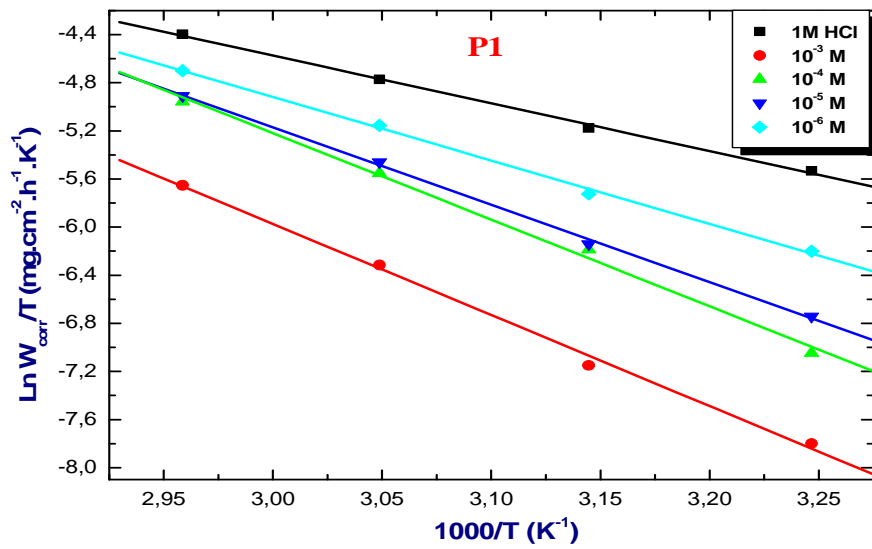


Figure 6. Arrhenius plots of mild steel in 1 M HCl at different concentrations of P1, P2 and P3



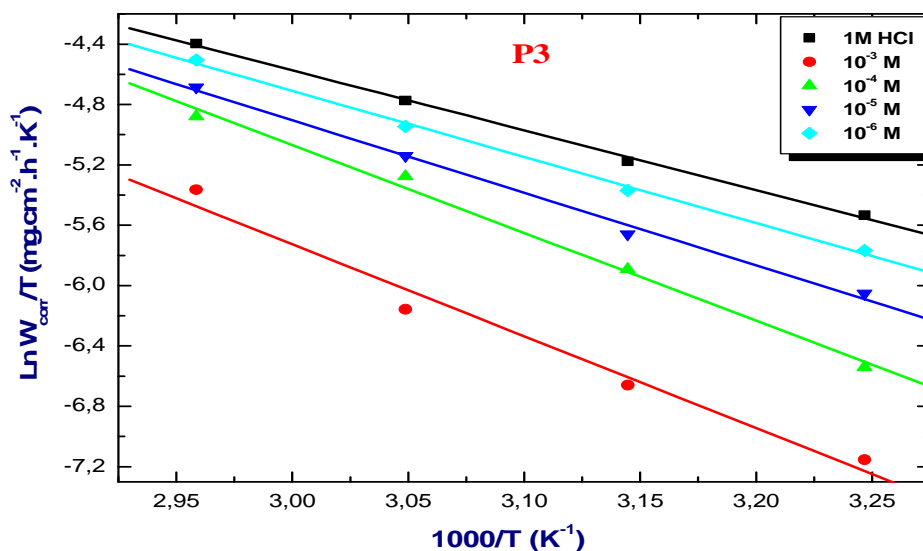


Figure 7. The relationship between $\ln W_{\text{corr}}/T$ and $1000/T$ for mild steel at different concentrations of P1, P2 and P3

The values of apparent activation energy (E_a) and pre exponential factor were calculated from the slop and intercept of the straight lines obtained in Arrhenus plots. The results are shown in Table 5. The Addition of inhibitors causes a rise in activation energy value when compared to the blank solution.

The lower value of E_a in inhibited solution when compared to that for uninhibited one show that strong hemisorptions bond between the inhibitor and the metal is highly probable. In the opposite case a physisorption can usually occur [28]. From Table 5, it appears that E_a of the inhibited metal dissolution can be higher as well as lower than that of the uninhibited reaction in case of a high degree of surface coverage. Hence, it can be suggested that the adsorption of benzoimidazopyridine onto mild steel surface can involve both physisorption and chemisorption.

Table 5. Activation parameters (activation energy (E_a), (ΔH^* and ΔS^*)) of the dissolution reaction of carbon steel in 1 M HCl in the absence and presence different concentrations of P1, P2 and P3

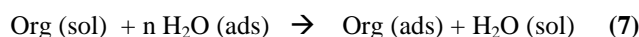
Concentration (M)	E_a (kJ.mol ⁻¹)			ΔH^* (kJ.mol ⁻¹)			ΔS^* (J.K ⁻¹ mol ⁻¹)		
--	35,67			32,99			-148,67		
	P1	P2	P3	P1	P2	P3	P1	P2	P3
10^{-3}	64,06	64,33	48,13	62,97	61,40	50,65	-70,39	-74,80	-105,30
10^{-4}	59,14	58,61	53,78	59,91	55,93	48,43	-73,26	-87,16	-106,47
10^{-5}	56,24	56,86	54,88	53,56	54,19	39,97	-91,93	-91,48	-130,47
10^{-6}	46,60	52,36	39,10	43,92	49,68	36,43	-118,73	-101,62	-139,50

The positive sign of enthalpies reflects the endothermic nature of the steel dissolution process meaning that the dissolution of carbon steel is more difficult. The entropy of activation ΔS^* in the absence of inhibitors is negative and this value increases with the inhibitors concentration. The increase of ΔS^* implies that an increase in disordering taking place on going from reactants to the activated complex [28].

3.3.2. Thermodynamic parameters of the adsorption process

The effect of addition of P1, P2 and P3 at different concentration on the corrosion of carbon steel in molar hydrochloric solution by weight loss at temperature range 298 to 338K.

The values of percentage inhibition efficiency %IE and the surface coverage θ are shown in The adsorption of organic inhibitors to the metal surface is a displacement reaction between these compounds in an aqueous phase and the water molecule on the surface of the metal



Org (sol) and Org (ads) are the organic molecules in the aqueous solution that adsorbed to the metal surface. While n is the number of water molecules replaced by one organic inhibitor [26, 29].

Table 6. The inhibition efficiency increase with increasing concentration, noting that P2 and P3 give good efficiency for the higher concentration $10^{-3}M$

Inhibitor	Concentration (M)	W_{corr} ($mg.cm^{-2}.h^{-1}$)	IE (%)	θ
1M HCl	00	0,6893	-	-
P1	10^{-3}	0,0670	92,21	0,922
	10^{-4}	0,0515	84,24	0,802
	10^{-5}	0,1324	79,04	0,790
	10^{-6}	0,1288	54,48	0,544
P2	10^{-3}	0,6893	91,61	0,916
	10^{-4}	0,1337	82,31	0,823
	10^{-5}	0,2202	78,41	0,784
	10^{-6}	0,1425	65,78	0,657
P3	10^{-3}	0,0761	88,26	0,882
	10^{-4}	0,1900	70,07	0,700
	10^{-5}	0,4153	66,87	0,668
	10^{-6}	0,1864	38,07	0,380

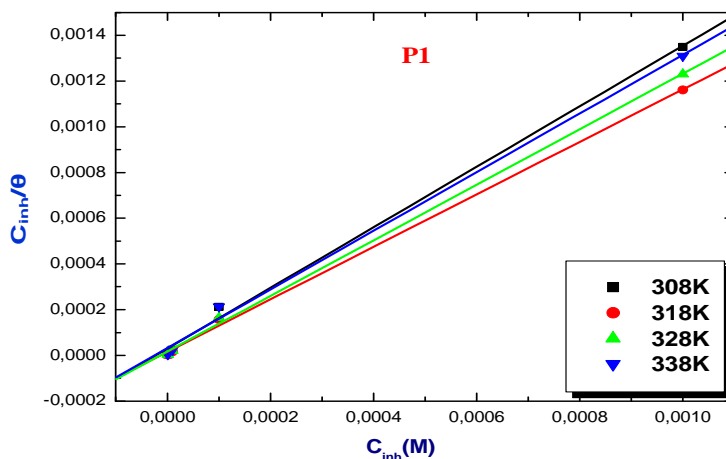
The values of surface coverage θ for different inhibitor concentrations were tested by fitting to various isotherms. The best fit was obtained with Langmuir isotherm (Figure 7). According to this isotherm, the surface coverage θ is related to the equilibrium adsorption constant K_{ads} and concentration of inhibitor [30]:

$$C_{inh}/\theta = 1/K_{ads} + C_{inh} \quad (8)$$

Where C_{inh} is the inhibitor concentration and K_{ads} is the equilibrium constant for the adsorption process. The values of C_{inh}/θ were plotted versus C_{inh} yields a straight line as shown in Fig. 4. These plots are linear with slope equal and regression coefficients R^2 almost equal to unity ($R^2 > 0.99$). The free adsorption energy is calculated from the equilibrium adsorption constant:

$$\Delta G_{ads}^0 = -RT \ln 55.5 K_{ads} \quad (9)$$

Where R is the gas constant, T is the temperature in K and the value of $55,55$ in the above equation is the concentration of water in solution in $mol L^{-1}$.



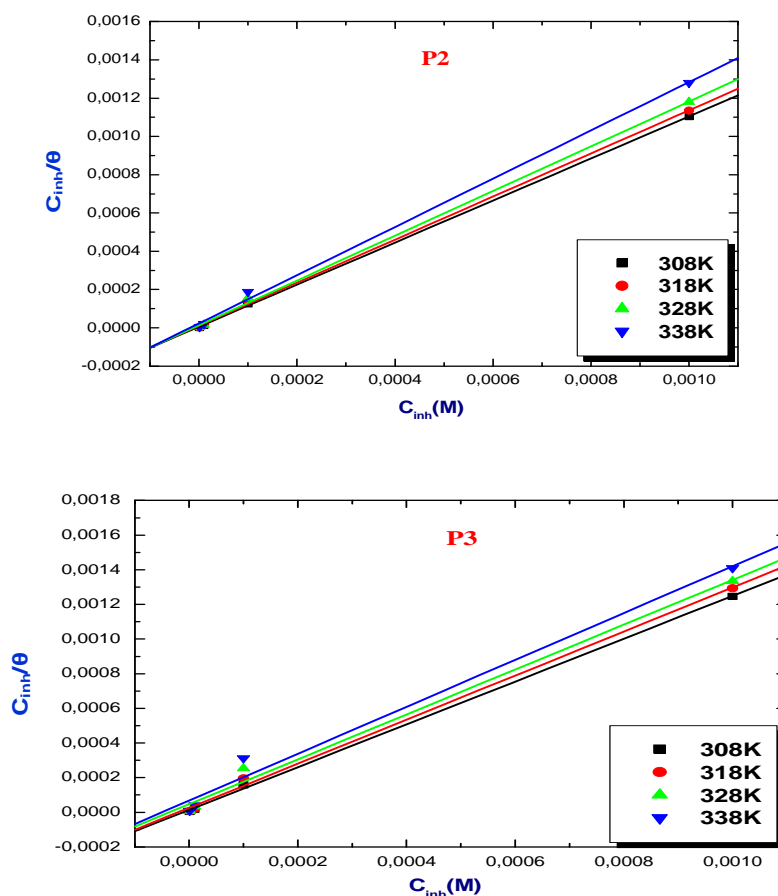


Figure 8. Langmuir adsorption plots for mild steel in 1 M HCl solution containing different concentration of P1, P2 and P3 at different temperature

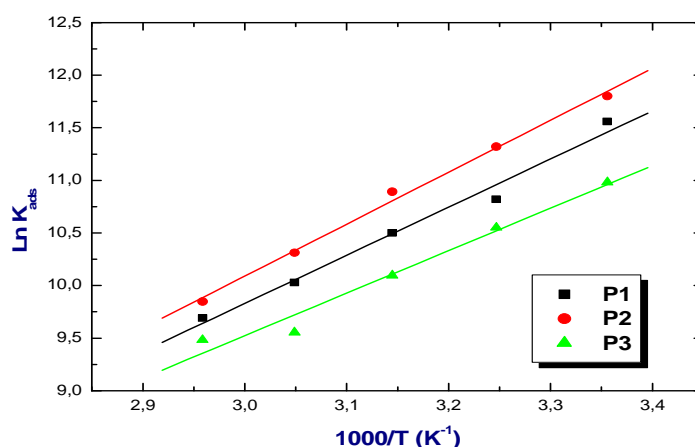
The calculated thermodynamic adsorption parameters K_{ads} and ΔG°_{ads} for all the studied compounds in 1.0 M HCl solutions are given in Table 7. The negative values of ΔG°_{ads} ensure the spontaneity of the adsorption process and stability of the adsorbed layer on the steel surface. Generally, values of ΔG°_{ads} up to -20 kJ/mol are consistent with the electrostatic interactions between the charged molecules and the charged metal (physisorption) while those around -40 kJ/mol or higher are associated with chemisorption [31]. The values of ΔG°_{ads} for P1, P2 and P3 are around -40 kJ/mol which indicates that this compounds involves two types of interaction with mostly chemisorption. The thermodynamic parameters ΔH°_{ads} and ΔS°_{ads} for the adsorption of the studied inhibitors on mild steel are calculated from the two equations:

$$\text{Van't Hoff [32]: } K = \frac{1}{55.5} \exp\left(\frac{-\Delta G^{\circ}_{ads}}{RT}\right) \quad (10)$$

$$\text{Gibbs-Helmholtz [33]: } \Delta G^{\circ}_{ads} = \Delta H^{\circ}_{ads} - T\Delta S^{\circ}_{ads} \quad (11)$$

Table 7. Thermodynamic parameters for the adsorption of P1, P2 and P3 on C38 steel at different temperatures

Inhibitor	Temperature (K)	K_{ads}	ΔG°_{ads} (KJ/mol)	ΔH°_{ads} (KJ/mol)	ΔS°_{ads} (KJ/mol)
P1	298	$1,79.10^5$	-39,94	-32,46	71,49
	308	$5,01.10^4$	-38,02		
	318	$2,43.10^4$	-37,34		
	328	$3,74.10^4$	-39,69		
	338	$3,98.10^4$	-41,08		
P2	298	$1,33.10^5$	-39,21	-39,37	74,52
	308	$8,25.10^4$	-39,30		
	318	$7,26.10^4$	-40,24		
	328	$2,47.10^4$	-38,55		
	338	$1,89.10^4$	-38,98		
P3	298	$5,88.10^4$	-37,18	-21,64	67,04
	308	$3,82.10^4$	-37,33		
	318	$2,42.10^4$	-37,33		
	328	$1,41.10^4$	-37,03		
	338	$1,31.10^4$	-37,95		

Figure 9. The relationship between $\ln(K_{ads})$ and $1000/T$ for mild steel at different concentrations of inhibitors

It is assumed that an exothermic process is attributed to either physical or chemical adsorption but endothermic process corresponds solely to chemisorption. In this study, the values calculated of inhibitors for both inhibitors are negatives ($-32,46$, $-39,37$ and -21.64 $\text{kJ}\cdot\text{mol}^{-1}$) for P1, P2 and P3 respectively, reflecting the exothermic behaviour of adsorption on the steel surface [34-35]. The negative values of ΔS°_{ads} is generally explained by an ordered of adsorbed molecules of inhibitor with the progress in the adsorption onto the mild steel surface [36]. The ΔS°_{ads} in presence of these compounds is large positive meaning that an increase in disordering takes places in going from reactants to the metal-adsorbed species reaction complex [37].

3.4. Scanning Electron Microscope (SEM)

Surface analyses for the corrosion of mild steel specimens in 1M HCl solution without and with inhibitors were carried out by SEM. Figure 10 and 11 represent the scanning electron microscopic (SEM) images of mild steel surface that has been exposed to the 1M HCl for 6h in the absence and presence of studied inhibitors, respectively.

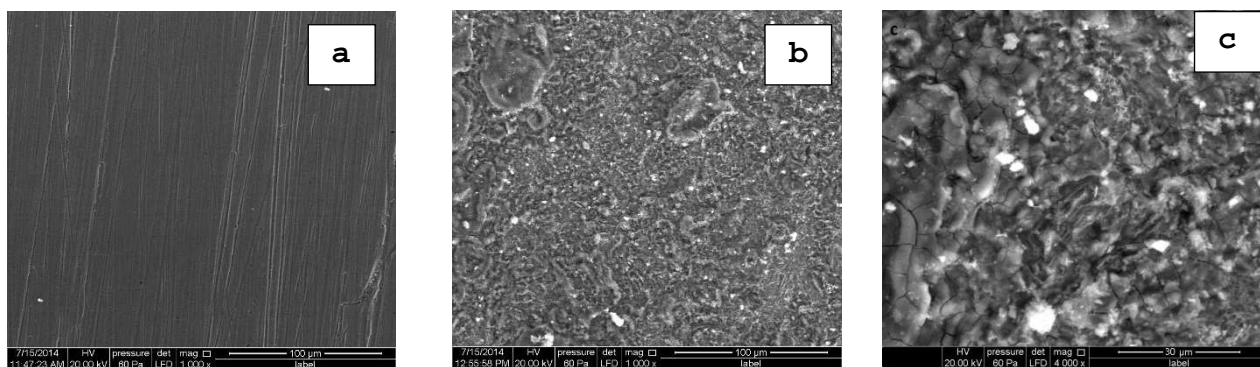


Figure 10: SEM image of mild steel surface (a) before immersion in 1M HCl, (b) and (C) after 6 hours of immersion in 1M HCl solution in the absence of inhibitors

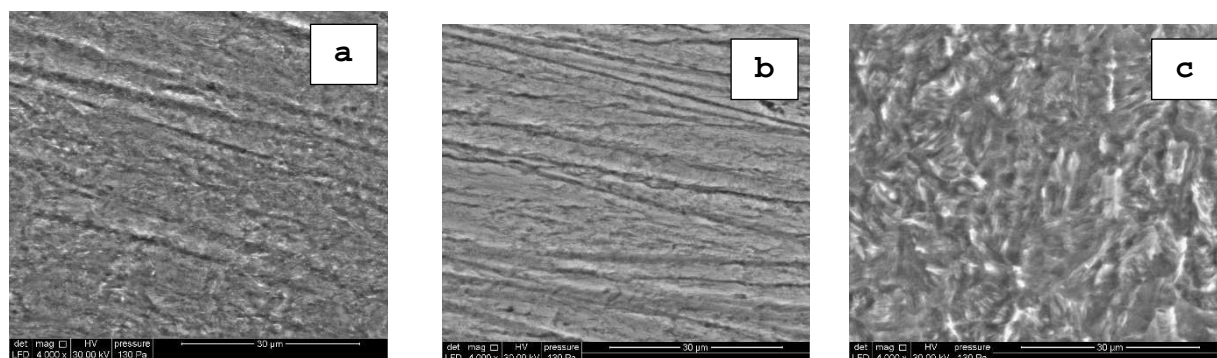


Figure 11. SEM image of mild steel after 6 hours of immersion in 1M HCl solution with 10^{-3} M of inhibitor P1 (a), P2 (b) and P3 (c)

SEM is an experiment that was performed to check if the test compounds are actually adsorbed on the surface of mild steel or simply peeled from the surface. Figures 10 and 11. Show SEM images of the carbon steel surface after treatment with 1 M HCl containing 10^{-3} M of studied inhibitors. From these images it is evident that the steel surface appears to be almost unaffected by corrosion. This is due to the adsorption of inhibitors studied forming a thin protective film of inhibitors on the metal surface. This film is responsible for the highly effective inhibition by these inhibitors.

CONCLUSION

The studied benzoimidazopyridine compounds have proved to be good inhibitors for mild steel corrosion in hydrochloric acid.

Good agreement between the data obtained from potentiodynamic polarization, electrochemical impedance spectroscopy and weight loss measurements.

The efficiency of the inhibitors increase with concentration (the maximum %IE was showed at 10^{-3} M in order P2 > P1 > P3) but decrease with temperature.

Tafel results indicate the studied inhibitors acts as mixed-type with predominantly cathodic. This is retarding both the cathodic process without changing the mechanism of corrosion process.

The results of EIS show that the use of P1, P2 and P3 significantly increase the charge transfer values and decrease the double layer capacitance. Suggesting that the adsorption led formation of a protective film on the surface of metal.

From weight loss the adsorption of all inhibitors on carbon steel surface is well described by the Langmuir adsorption isotherm. All the values of E_a of the inhibited metal dissolution can be higher as well as lower than that of the uninhibited reaction in case of a high degree of surface coverage. Hence, it can be suggested that the adsorption of benzoimidazopyridine onto mild steel surface can involve both physisorption and chemisorption.

ΔG_{ads}° are around -40 kJ/mol which indicates that these compounds involve two types of interaction with mostly chemisorption. ΔH_{ads}° for the studied inhibitors are slightly less than -40 kJ mol⁻¹ may suggest chemisorption.

⇒ These results confirm that both chemisorption and physisorption mechanism.

REFERENCES

- [1] Y. Jianguo, W. Lin, V. Otteno-Alego and D.P. Schweinsberg, *Corros. Sci.*, **1995**, 37, 975.
- [2] F. El-Hajjaji, R.A. Belkhemima, B. Zerga, M. Sfaira, M. Taleb, M. Ebn Touhami, B Hammouti. S.S. Al-Deyab, E. Ebenso, *Int. J. Electrochem. Sci.*, **2014**, 9, 4721 – 4731
- [3] K. Adardour, O. Kassou, R. Tourir, M. Ebn Touhami, H. ElKafsaoui, H. Benzeid, El M. Essassi, M. Sfaira, *J. Mater. Envir. Sci.*, **2010**, 1, 129.
- [4] R. Salghi, D. Ben Hmamou, O. Benali, S. Jodeh, I. Warad, O. Hamed, Eno. E. Ebenso, A. Oukacha, S. Tahrouch, B. Hammouti, *Int. J. Electrochem. Sci.*, **2015**, 10, 8403-8411.
- [5] D. Bouzidi, A. Chetouani, B. Hammouti, S. Kertit, M. Taleb, S.S. Al-Deyab, *Int. J. Electrochem. Sci.*, **2012**, 7, 2334 – 2348
- [6] M. Zerfaoui, B. Hammouti, H. Oudda, M. Benkaddour, S. Kertit, *Bull. Electrochem.*, **2004**, 20, 433.
- [7] A.Y. Musa, A.A.H. Kadhun, A.B. Mohamad, M.S. Takriff, A.R. Daud, S.K. Kamarudin, *Corr. Sci.*, **2010**, 52, 526.
- [8] A.S.Fouda, K.Shalabi, H.Elmgazy, *J. Mater. Environ. Sci.* **2014**, 5, 1691-1702.
- [9] S. Aloui, I.Forsal, M. Ebn Touhami, M. Taleb, M.F. Baba, M. Daoudi, Portugaliae, *Electrochim.Acta*, **2009**, 27, 599.
- [10] R. Karthik, P. Muthukrishnan, Shen-Ming Chen, B. Jeyaprabha, P. Prakash, *Int J Electrochem Sci.*, **2015**, 10.
- [11] A. Zarrouk, B. Hammouti, H. Zarrok, M. Bouachrine, K.F. Khaled, S.S. Al-Deyab, *Int. J. Electrochem. Sci.*, **2012**, 7, 89.
- [12] S. El Arrouji, K. Ismaily Alaoui, A. Zerrouki, S. EL Kadiri, R. Touzani, Z. Rais, M. Filali Baba, M. Taleb, F. El-Hajjaji, A. Chetouani, A. Aouniti, *J. Mater. Environ. Sci.*, **2016**, 7(1), 299-309.
- [13] W.Li, Q.He, C. Pei, B. Hou, *Electrochem. Acta*, **2007**, 52, 6386.
- [14] M.Ellouz, N. K.Sebbar, H.Elmsellem, H.Steli, I.Fichtali, M. M.Mohamed Abdelahi, K.Al Mamari, E. M.Essassi, I.Abdel-Rahaman, *J. Mater. Environ. Sci.*, **2016**, 7 (8), 2806-2819
- [15] I. Ahamad, M. A. Quraishi, *Corros. Sci.*, **2010**, 52, 651–656.
- [16] A. Aouniti, R. Mokhlisse, S. Kertit, K. Elkacemi, *Ann. Chim. Sci. Mat*, **2000**, 25, 437-446.
- [17] N. Abdulwali, F. Mohammed, A. Al subari, H. Ghaddar, A. Guenbour, A. Bellaouchou, E. M. Essassi, *Int. J. Electrochem. Sci.*, **2014**, 9, 6402 – 6415.
- [18] F. -Z.Qachchachi, Y.Kandri Rodi, H.Elmsellem, H.Steli, A.Haoudi, A. Mazzah, Y.Ouzidan, N. K.Sebbar, E. M.Essassi, *J. Mater. Environ. Sci.*, **2016**, 7 (8), 2897-2907.
- [19] H.Elmsellem, A.Aouniti, Y. Toubi, H. Steli, M. Elazzouzi, S. Radi, B. Elmahi, Y. El Ouadi, A. Chetouani, B. Hammouti, *Der Pharma Chemica*, **2015**, 7(7), 353-364.
- [20] A. Popova, E. Sokolova, S. Raicheva, M. Christov, *Corros. Sci.*, **2003**, 45, 33–55.
- [21] A. Popova, M. Christov, S. Raicheva, E. Sokolova, *Corros. Sci.* **2004**, 46, 1333–1350.
- [22] K. Hnini, S.Fadel, M. A. EL Mhammedi, A. Chtaini, E. Rakib, *Leonardo Electronic Journal of Practices and Technologies*, ISSN 1583-1078.
- [23] R. Karthik, P. Muthukrishnan, Shen-Ming Chen, B. Jeyaprabha, P. Prakash *Int. J. Electrochem. Sci.*, 10 (2015) 3707 – 3725
- [24] A.S.Patel, V.A.Panchal, P.T.Trivedi and N.K.Shah, *Organic Schiff*, **2012**, 30, 3163.
- [25] H. H. Uhlig, *Corrosion and Corrosion Control 2nd Ed.*, John Wiley and sons Inc. **1997**.
- [26] K. Ismaily Alaoui F. Ouazzani, Y. kandri rodi, A.M. Azaroual, Z. Rais, M. Filali Baba, M. Taleb, A. Chetouani, A. Aouniti, B. Hammouti, *J. Mater. Environ. Sci.*, **2016**, 7 (1), 244-258.
- [27] M.Messali, A. Bousskri, A. Anejjar, R. Salghi, B. Hammouti *Int. J. Electrochem. Sci.*, **2015**, 10, 4532-4551.
- [28] A.Abd-El-Nabey, E.Khamis, M. S.Ramadan, A.El-Gindy, *Corrosion*, **1996**, 52, 671.
- [29] H. Elmsellem, T. Harit, A. Aouniti, F.Malek, A. Chetouani, B. Hammouti, *Protection of Metals and Physical Chemistry of Surfaces*, A, **2015**, 51(5), 873–884.
- [30] R. Karthikaiselvi, S. Subhashini, *Journal of the Association of Arab Universities for Basic and Applied Sciences*, **2014**, 16, 74–82.
- [31] N. K. Sebbar, H. Elmsellem, M. Boudalia, S. Iahmidi, A. Bellaouchou, A. Guenbour, E. M. Essassi, H. Steli, A. Aouniti, *J. Mater. Environ. Sci.*, **2015**, 6 (11), 3034-3044.
- [32] G.K. Jennings, P.E. Laibinis, *Colloids Surf. A*, **1996**, 116, 105.
- [33] Z. Zhang, S. Chen, Y. Li et al., *Corros. Sci.*, **2009**, 51, 291.
- [34] B. Zerga, B. Hammouti, M. Ebn Touhami, R. Tourir, M. Taleb, M. Sfaira, M. Bennajeh, I. Forssal *Int. J. Electrochem. Sci.*, **2012**, 7, 471 – 483.

- [35] M. Belayachi, H. Serrar , H. Zarrok , A. El Assry , A. Zarrouk , H. Oudda, S. Boukhris, B. Hammouti , Eno E. Ebenso , A. Geunbour *Int. J. Electroch. Sci*, **2015**, *10*,3010-3025.
- [36] W.Niouri, B. Zerga, M. Sfaira, M. Taleb, M. Ebn Touhami, B. Hammouti, M. Mcharfi, S.S. Al-Deyab, H. Benzeid, El M. Essassi *Int. J. Electrochem. Sci*, **2014**, *10*, 8283 – 8298.
- [37] H.-L.Wang, H.-B Fan, J.-S.Zheng, *Mater. Chem. Phys*, **2002**, *77*, 655.